Neuropilin–Semaphorin III/D-Mediated Chemorepulsive Signals Play a Crucial Role in Peripheral Nerve Projection in Mice

Takashi Kitsukawa,*§ Masayuki Shimizu,*
Makoto Sanbo,‡ Tatsumi Hirata,*
Masahiko Taniguchi,†‡ Yoko Bekku,*
Takeshi Yagi,‡ and Hajime Fujisawa*‖
*Group of Developmental Neurobiology
Division of Biological Science
Nagoya University Graduate School of Science
Chikusa-ku, Nagoya 464-01
Japan
†Department of Morphology
Institute for Developmental Research
Aichi Human Service Center
Kamiya, Kasugai, Aichi 480-03
Japan
‡Laboratory of Neurobiology and Behavioral Genetics
National Institute for Physiological Science
Myodaiji, Okazaki 444
Japan

Summary

Neuropilin is a neuronal cell surface protein and has been shown to function as a receptor for a secreted protein, semaphorin III/D, that can induce neuronal growth cone collapse and repulsion of neurites in vitro. The roles of neuropilin in vivo, however, are unknown. Here, we report that neuropilin-deficient mutant mice produced by targeted disruption of the neuropilin gene show severe abnormalities in the trajectory of efferent fibers of the PNS. We also describe that neuropilin-deprived dorsal root ganglion neurons are perfectly protected from growth cone collapse elicited by semaphorin III/D. Our results indicate that neuropilin–semaphorin III/D-mediated chemorepulsive signals play a major role in guidance of PNS efferents.

Introduction

During development, nerve fibers grow for long distances toward their targets to give rise to fairly stereotyped patterns of nerve fiber tracts and connections. Among several mechanisms responsible for neuronal connections (for review, see Goodman and Shatz, 1993), the directional growth of axons with a high degree of precision seems primarily important to generate frameworks of neuronal connections. In vertebrate peripheral nervous systems (PNSs), sensory and motor neuron efferent fibers are fasciculated into the cranial or spinal nerves in highly specific and segmental manners, follow discrete paths within embryos, and eventually innervate muscles or skin at appropriate regions. Several lines of study, mostly on the limb innervation in chick embryos (Lance-Jones and Landmesser, 1980; Scott, 1986; Tosney, 1988; Lance-Jones and Dias, 1991; Tang et al., 1992; Rafuse et al., 1996), have shown that selective axon

§Present address: Laboratory of Specification Mechanisms 1, National Institute for Basic Biology, Myodaiji, Okazaki 444, Japan.
‖To whom correspondence should be addressed.

fasciculation and responsiveness of neuronal growth cones to local guidance signals are the essential mechanisms in the initial step of PNS efferent projection. Despite these extensive studies, however, little is known about the molecular mechanisms underlying fasciculation or guidance of the PNS efferent fibers.

Over the past decade, a variety of molecules involved in nerve fiber fasciculation and guidance have been identified in both invertebrates and vertebrates; some serve as cell adhesion receptors (for reviews, see Rutishauser and Jessell, 1988; Goodman and Shatz, 1993), and others are attractive or repulsive guiding cues that may promote or arrest the advance of neuronal growth cones (for reviews, see Goodman, 1996; Tessier-Lavigne and Goodman, 1996). Among these, collapsin-1 in the chicken (Luo et al., 1993) and its mammalian homolog, semaphorin III/D, (Kolodkin et al., 1993; Püschel et al., 1995) are potent chemorepellents that can repel or collapse growth cones of dorsal root ganglion (DRG) neurons in vitro (Luo et al., 1993; Fan and Raper, 1995; Messersmith et al., 1995; Püschel et al., 1995, 1996; Shepherd et al., 1997; Varela-Echavarria et al., 1997) and have been suggested to be repulsive guidance signals for DRG fibers. However, the role of the chemorepellents in PNS fiber guidance in vivo is still unknown.

Neuropilin (formerly A5 or A5 protein; Takagi et al., 1987, 1991) is a type I membrane protein that is highly conserved among vertebrates, including Xenopus laevis (Takagi et al., 1987, 1991), chicken (Takagi et al., 1995), and mice (Kawakami et al., 1996). Neuropilin is expressed in particular classes of neurons: in the mouse PNS, neuropilin is expressed in the trigeminal, facial, glossopharyngeal, and vagus nerves, and in the spinal sensory and motor nerves (Kawakami et al., 1996). Neuropilin protein is restrictively localized on growing axons and growth cones (Fujisawa et al., 1995; Takagi et al., 1995; Kawakami et al., 1996). Neuropilin is a molecule that can mediate cell adhesion by a heterophilic molecular interaction (Takagi et al., 1995) and can promote neurite outgrowth in vitro (Hirata et al., 1993). In Xenopus tadpoles, neuropilin is expressed in the olfactory axon subclasses and has been suggested to play a role in selective fasciculation of the axons (Satoda et al., 1995). Furthermore, ectopic and excess expression of neuropilin in mouse embryos induced defasciculation and abnormal sprouting of PNS fibers (Kitsukawa et al., 1995). These observations suggest the importance of neuropilin in axon growth, fasciculation, or guidance. More recently, two expression cloning studies have shown that neuropilin is a semaphorin III/D-binding protein and mediates semaphorin III/D-induced chemorepulsive signals to DRG neurons (He and Tessier-Lavigne, 1997; Kolodkin et al., 1997). These results suggest that neuropilin is a receptor or a component of a receptor complex for semaphorin III/D. However, the roles of neuropilin, particularly in vivo, have not been defined.

Here, we produced neuropilin-null mutant mice by targeted disruption of the neuropilin gene and clarified the function of neuropilin in the development of the nervous system. The neuropilin mutant mice were embryonic lethal. Live homozygous mutant embryos could
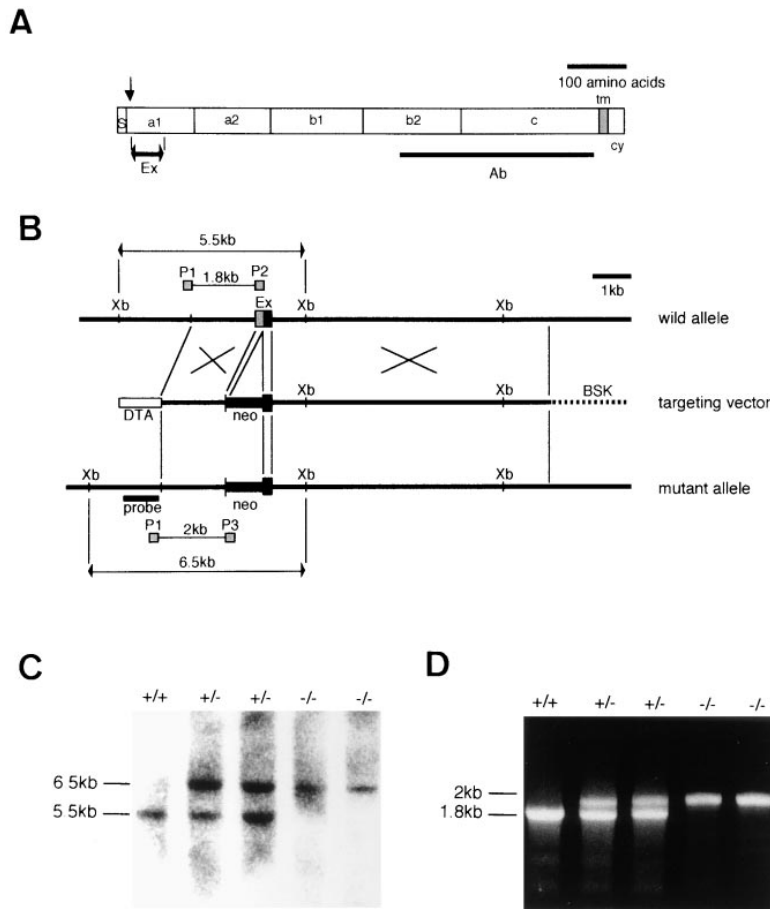
A

B

C

D

Figure 1. Targeted Disruption of the Neuropilin Gene

(A) Domain structure of the mouse neuropilin protein. Signal peptide (S), domains in the extracellular part of the protein (a1, a2, b1, b2, c), transmembrane domain (tm), and cytoplasmic domain (cy) are shown. Ex, the exon isolated (see below); arrow, the site of interruption by the targeted disruption of the neuropilin gene (see below); Ab, the region to which the antibody was generated (see Kawakami et al., 1996).

(B) Neuropilin gene targeting strategy (see Experimental Procedures for details). Native neuropilin gene (top), the targeting vector (middle), and the disrupted neuropilin gene (bottom) are shown. The box in the wild allele indicates the exon encoding the N-terminal half of the a1 domain (see [A]). The 5′ half of the exon was deleted (stippled part). neo, PGK-neo cassette; DTA, diphtheria toxin A fragment gene cassette; Xb, XbaI; BSK, Bluescript SK.

(C) Southern blotting analysis of embryos derived from neuropilin heterozygous intercrosses. Genomic DNA was digested with XbaI and probed with the 5′ flanking probe shown in (B). Expected sizes of DNAs of the wild-type and mutant alleles (5.5 kb and 6.5 kb, respectively) are indicated in (B).

(D) PCR analysis of DNA from the embryos as shown in (C) with primers P1 and P2 in the deleted part of the exon (see [B]) and with P1 and P3 in the neomycin resistance gene (see B). Expected sizes of amplified DNAs (1.8 kb for the P1 and P2 primers and 2 kb for the P1 and P3 primers) are indicated in (B).

be observed as late as 12.5 days postcoitus (dpc) and showed severe abnormalities in the trajectory of the cranial and spinal efferent fibers that express neuropilin in normal embryos. We also showed that DRG growth cones of the neuropilin mutants were protected from the semaphorin III/D-induced collapse. These results indicate that neuropilin is a functional receptor or an indispensable component of a receptor complex for the growth cone repellent semaphorin III/D, and neuropilin–semaphorin III/D-mediated chemorepulsive signals are essential in directional guidance of PNS efferent fibers in vivo.

Results

Generation of Neuropilin Mutants

Targeting strategies for the neuropilin gene and genotype analyses of mice are summarized in Figure 1. To inactivate the functions of neuropilin completely, we isolated an exon that encodes the N-terminal half of the a1 domain of the mouse neuropilin protein (Figure 1A), deleted the 5′ half of the exon, then inserted the neomycin resistance gene (neo) out of frame into the deleted exon. Thus, the mutated allele produced by homologous recombination was expected to encode only the signal peptide and the most N-terminal 7 amino acid residues of the neuropilin protein. Southern blotting (Figure 1C) and polymerase chain reaction (PCR; Figure 1D) analyses indicated successful homologous recombination of

the neuropilin gene. Immunohistochemical analysis of homozygous mutant embryos with antibodies generated against a fusion protein corresponding to the b2 and c domains of the neuropilin protein (Figure 1A; see Kawakami et al., 1996) showed no positive staining (data not shown), confirming that the mutant embryos lacked intact neuropilin protein.

We created neuropilin heterozygous mice by crossing germline chimeric mice with C57BL/6 or ICR females. After two to three backcross generations, we obtained homozygous mice by intercrossing the heterozygous offspring. The homozygous mice always died in utero. In the C57BL/6 genetic background, all homozygous embryos died as early as 10.5 dpc, while in the ICR genetic background, live homozygous embryos could still be observed as late as 12.5 dpc, but no viable homozygous embryos were seen by 13.5 dpc. This embryonic death was probably attributable to anomalies in the cardiovascular system (unpublished data). In this study, all analyses were performed on neuropilin mutants produced in the ICR genetic background.

Abnormal Trajectory of Cranial Nerve Fibers in Neuropilin Mutants

Homozygous neuropilin mutant embryos up to 12.5 dpc exhibited nearly normal external appearances. However, immunostaining of the mutant embryos with an anti-neurofilament antibody 2H3 (Dodd et al., 1988) in whole-mount preparations (three embryos [three dams], four
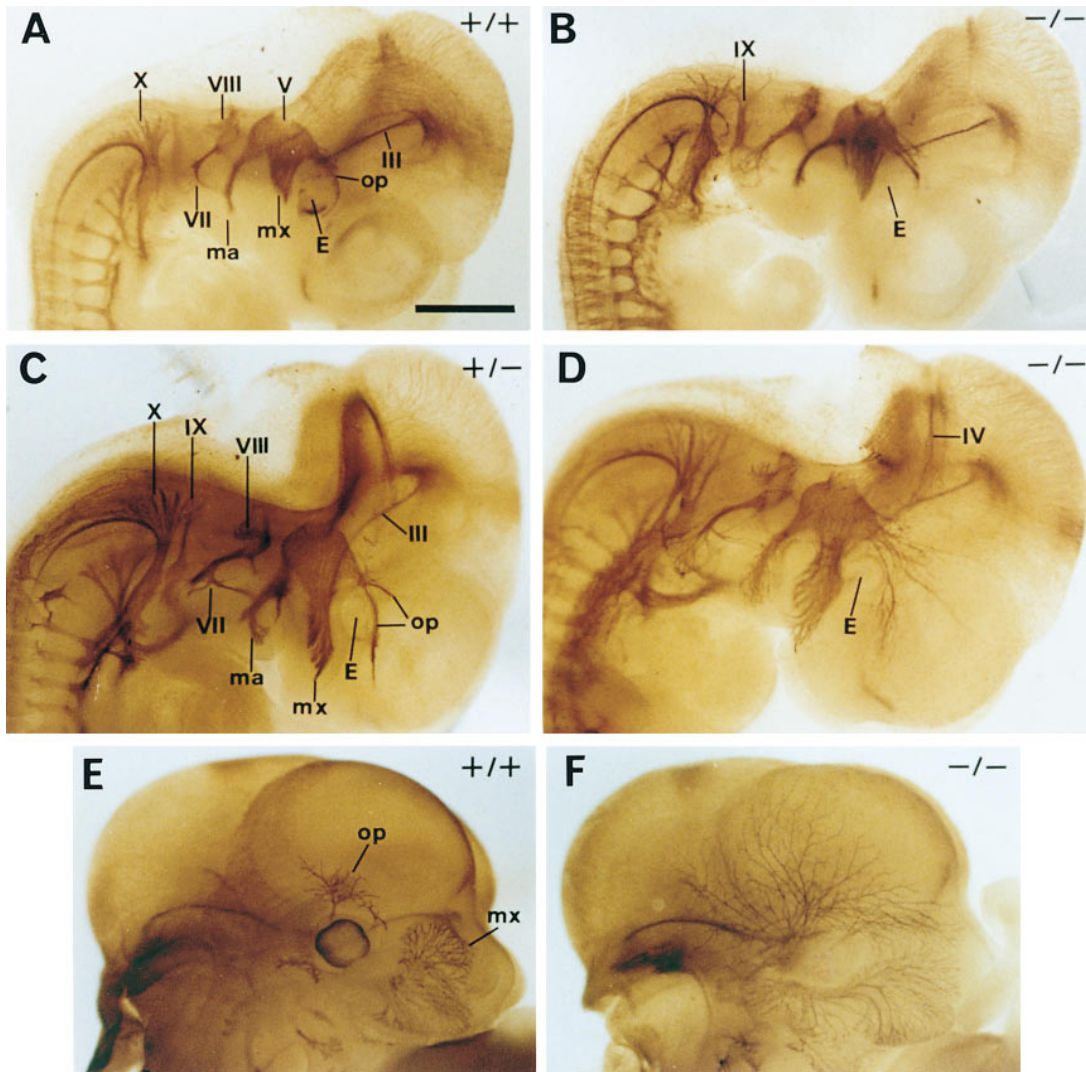
Figure 2. Pathway and Projection of Cranial Nerves

Whole-mount immunostaining with anti-neurofilament monoclonal antibody 2H3 of the wild-type (+/+), heterozygous (+/−), and homozygous mutant (−/−) embryos at 9.5 dpc (A and B), 10.5 dpc (C and D), and 12.5 dpc (E and F). III, oculomotor nerve; IV, trochlear nerve; V, trigeminal nerve; VII, facial nerve; VIII, vestibulocochlear nerve; IX, glossopharyngeal nerve; X, vagus nerve; op, ophthalmic nerve; mx, maxillary nerve; ma, mandibular nerve, E; eye. Eye pigmentation differed from embryo to embryo because the chimeric mice that were produced using TT-2 ES cells were crossed with ICR mice. Scale bar (in [A]), 1 mm for (A)–(F).

embryos [three dams], and eight embryos [four dams] at 9.5 dpc, 10.5 dpc, and 12.5 dpc, respectively) or sections (three embryos [three dams], six embryos [five dams], and 15 embryos [ten dams] at 9.5 dpc, 10.5 dpc, and 12.5 dpc, respectively) exhibited severe abnormalities in both the cranial and spinal nerves.

In the neuropilin mutant embryos, the positions and size of the cranial ganglia of the trigeminal, glossopharyngeal, and vagus nerves were almost normal (Figures 2A–2D). Moreover, all the cranial nerves projected to their correct target regions: the ophthalmic, maxillary, and mandibular branches of the trigeminal nerve projected to the frontal part of the head, the maxillary process, and mandibular process, respectively. The facial and glossopharyngeal nerves arrived at the second and third pharyngeal arches, respectively.

The trajectory of each cranial nerve, however, was severely disorganized in the neuropilin mutant embryos. In the embryos at 9.5 dpc, the ophthalmic nerve did not form a thick fiber bundle as found in the wild-type or heterozygous littermates but was separated into several fiber fascicles (compare Figures 2A and 2B). At 10.5 dpc, the ophthalmic nerve in the homozygous mutant embryos was further defasciculated and widely spread in the frontal part (compare Figures 2C and 2D). At 12.5 dpc, the ophthalmic nerve of the homozygous mutant embryos further expanded and overshot far beyond the growing front of the normal nerve within the front nasal part (compare Figures 2E and 2F). The distal parts of the maxillary and mandibular nerves were also defasciculated in the homozygous mutant embryos at 10.5 dpc (compare Figures 2C and 2D) and spread into almost

all parts of the maxillae and mandibula, respectively, at 12.5 dpc (compare Figures 2E and 2F). The distal parts of the facial nerve (Figures 2B and 2D), glossopharyngeal (Figure 2B), and vagus nerves (Figure 2B) in the homozygous mutant embryos also expanded.

Abnormalities in the pathway and trajectory of the cranial nerves described above were observed in all homozygous mutant embryos examined but not in the heterozygous ones. It is worth noting that, in the homozygous mutant embryos, defasciculation or excess spreading of nerve fibers was apparent in the cranial sensory and motor nerves in which neuropilin is expressed in normal embryos (Kawakami et al., 1996). In the present analysis on whole-mounted specimens, no abnormal pathway or trajectory was observed in the oculomotor, trochlear, or vestibulocochlear nerves, which originally lack neuropilin expression (see Figures 2B and 2D), even though further detailed analyses are necessary to determine the terminal patterns of these nerves.

Abnormal Trajectory and Projection of Spinal Nerve Fibers at Trunk Level in Neuropilin Mutants

We have shown that the spinal nerves of both the sensory and motor nerves are the normal sites of neuropilin expression (Kawakami et al., 1996). As shown in the scheme in Figure 3A and also by whole-mount immunostaining of wild-type or heterozygous mouse embryos with 2H3 (Figures 3C, 3E, and 3G), the pathway and projection of the spinal nerves were highly stereotyped and segmented. The main spinal nerve trunk was divided into the ramus dorsalis (rd in Figure 3A) and ramus ventralis (rv in Figure 3A). The ramus dorsalis turned dorsolaterally and formed muscle branches to the dorsal muscle groups and skin sensory rami (the lateral branches: lb in Figure 3A and arrowheads in Figures 3E and 3G) in a highly segmental pattern. The rami ventralis ran ventrally and sprouted the lateral cutaneous branches (lcb in Figure 3A and arrows in Figures 3E and 3G) toward the lateral body wall.

The patterned pathway and projection of the spinal nerves were severely disrupted in the neuropilin mutants. In the homozygous mutant embryos, DRGs showed loose cell packaging (Figures 3B and 3D), even though the number of DRG and their location within embryos were normal. The main spinal nerve trunks were partially defasciculated (compare Figures 3C and 3D), and several 2H3-positive fibers left the main spinal nerve trunks at arbitrary points (Figures 3D and 3F) or protruded directly from DRGs (Figure 3B) then grew into the skin surface in an irregular manner (Figure 3H). The segmental pattern of skin sensory innervation found in the normal embryos was partially but not completely disrupted in the neuropilin mutant embryos (compare Figures 3G and 3H). Several nerve fibers arrived at the opposite side of the embryos after crossing the dorsal midline (Figures 3H and 3I). No nerve fibers crossed the dorsal midline in the wild-type or heterozygous embryos (Figure 3G). All neuropilin mutant embryos examined showed similar phenotypes.

The dorsal root afferent that projects to the spinal cord also expresses neuropilin (Takagi et al., 1995; Kawakami et al., 1996). However, in the neuropilin mutant embryos up to 12.5 dpc, the dorsal root afferent arrived at correct positions within the spinal cord and formed the dorsal funiculus (Figures 3D, 3F, 3H, and 3I). Labeling of the dorsal root afferent fibers with the lipophilic dye DiI revealed no apparent abnormality in the trajectory of the fibers within the dorsal funiculus (data not shown).

Abnormal Limb Innervation in Neuropilin Mutants

In the wild-type and heterozygous embryos, the fourth to eighth cervical spinal nerves and part of the first thoracic spinal nerve once converged into a plexus (the branchial plexus) at the proximal part of the forelimb and then were segregated into the major dorsal and ventral nerve trunks within the limbs (see scheme in Figure 3A and Figures 3C and 3E). The major dorsal and ventral nerve trunks grew further along particular routes within the limbs and sprouted skin sensory rami at discrete points (Figure 4A). In the neuropilin mutant embryos, the convergence of the spinal nerves into the branchial plexus was reduced (compare Figures 3C and 3D), and each spinal nerve fiber innervated the limbs almost independently (Figure 3F). Within the limbs, the spinal nerve fibers were globally separated into dorsal and ventral groups (Figure 3B) but never formed thick nerve fiber bundles corresponding to the major dorsal or ventral nerve trunks observed in the wild-type or heterozygous embryos (compare Figures 3E and 3F). At 12.5 dpc, the neuropilin-deficient spinal nerves were distributed widely within the forelimbs (compare Figures 4A and 4B). The trajectories of spinal nerve fibers toward the hind limbs were also disorganized: spinal nerve fibers were poorly converged into either the crural or sciatic plexus (data not shown) and completely defasciculated within the limbs (compare Figures 4C and 4D). Similar abnormalities were observed in all mutant embryos examined.

To clarify the limb innervation pattern in detail, we filled spinal nerve fibers of the forelimbs with fluorescein-conjugated dextran and then examined the positions of DRG neurons and spinal motor neurons that had been retrogradely labeled with the tracer. As fluorescein-conjugated dextran is preferentially incorporated into severed fibers, a local incision of the forelimb and following application of the tracer enabled us to fill specific groups of fibers and to detect their somata within the spinal cord or DRGs. First, to test whether motor axons in the neuropilin mutant embryos overshoot to the skin surface, we peeled off the epidermis and a part of the dermis of either the dorsal or ventral surface of the forelimbs at the upper and lower arm levels and applied the tracer. In all specimens examined (five wild-type, four heterozygous, and two homozygous mutant embryos collected from two dams), sensory neurons in DRGs but not motor neurons in the spinal cord were labeled with the tracer (Figures 5A and 5B), suggesting that motor axons in the neuropilin mutant embryos are located at deeper parts of the forelimbs as in the wild-type embryos. Second, to test whether segregation of the spinal nerve fibers into the dorsal and ventral nerve fiber groups normally occurs within the forelimbs of the neuropilin mutants, we made a deep incision at the upper arm level of the dorsal or ventral parts of the forelimbs of either side and applied the tracer. In this study,
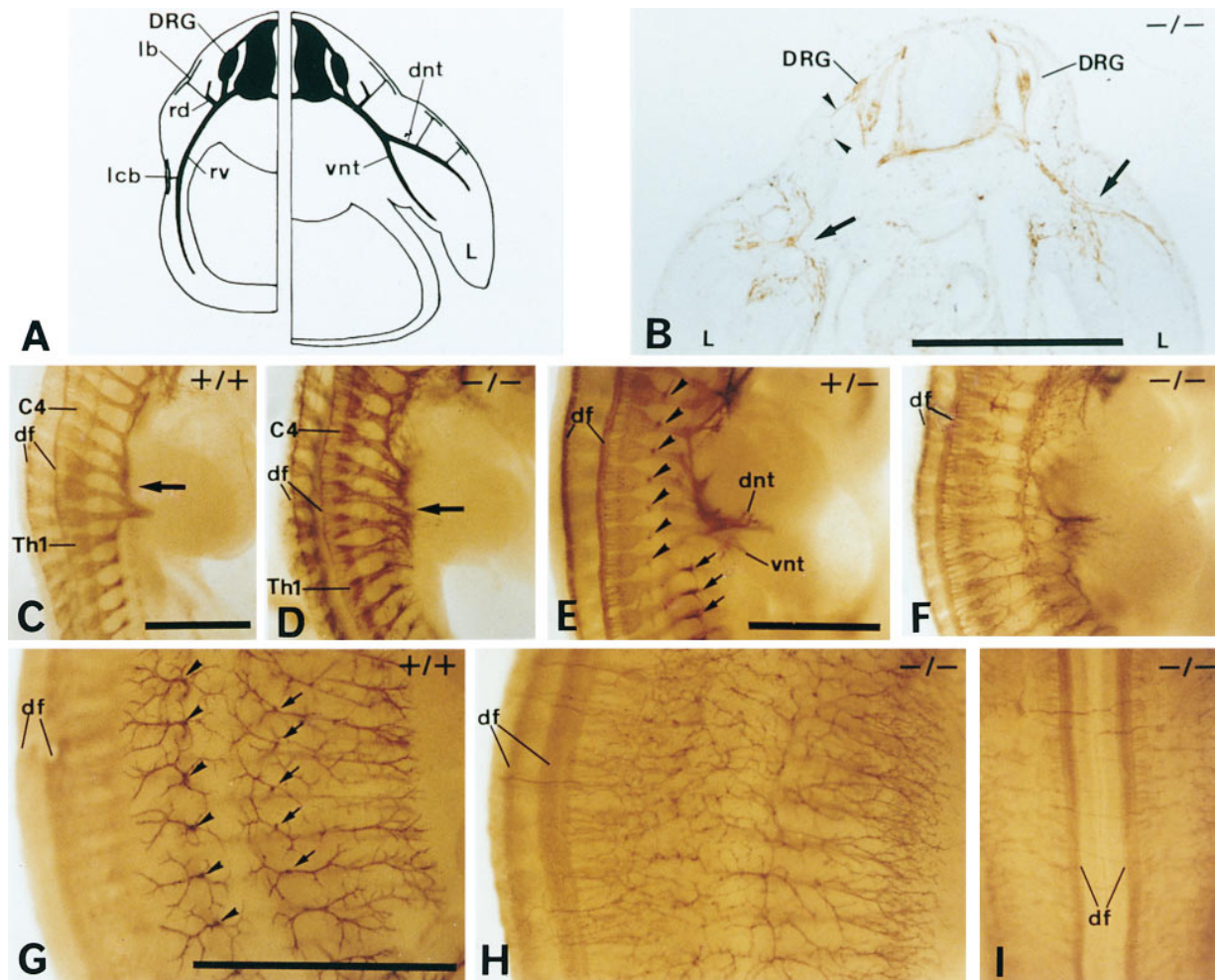
Figure 3. Pathway and Projection of Spinal Nerves at Trunk Level

Immunostaining with 2H3 of the wild-type (+/+), heterozygous (+/−), and homozygous mutant (−/−) embryos in sectioned (B) and whole-mounted specimens (C–I).

(A) Schemes representing spinal nerve pathways in the wild-type mouse embryo at the trunk level (left) and at the forelimb level (right). rd, ramus dorsalis; rv, ramus ventralis; lb, lateral branch; lcb, lateral cutaneous branch; dnt, dorsal nerve trunk; vnt, ventral nerve trunk; L, forelimb.

(B) A frontal section of a homozygous mutant embryo at 10.5 dpc. Arrowheads indicate fibers sprouting directly from the dorsal root ganglion (DRG). Arrows indicate the branchial plexus at the proximal part of the forelimbs (L).

(C–I) Trunk regions of embryos at 9.5 dpc (C and D), 10.5 dpc (E and F), and 12.5 dpc (G–I). (C)–(H), dorsolateral views; (I), dorsal view of the embryo in (H). Arrows in (C) and (D) indicate the branchial plexus. Arrowheads and arrows in (E) and (G) indicate penetration points of the lateral branches and the lateral cutaneous branches (see Figure 3A), respectively. C4, the fourth cervical nerve; Th1, the first thoracic nerve; df, the dorsal funiculus; dnt and vnt, the dorsal and ventral nerve trunks of the spinal nerves within the forelimbs, respectively. Scale bars (in [B], [C], [E], [G]), 1 mm. Figures in (C) and (D), (E) and (F), (G)–(I) are the same magnification, respectively.

we examined seven wild-type, six heterozygous, and four homozygous mutant embryos collected from two dams in which dorsal or ventral fibers within the limbs had been selectively filled with the tracer. In the wild-type mouse embryos, the motor neuron pools for either the dorsal and ventral nerve fiber groups of the forelimbs were not so locally segregated within the spinal cord (Figure 5C) as in chick embryos (Tsuchida et al., 1994), impeding detailed analyses of the segregation pattern of the fibers. Nonetheless, the distribution pattern of either the dorsal or ventral motor neuron groups was not clearly different at any level of the spinal cord between the wild-type and mutant embryos (Figures 5C and 5D), even though some homozygous mutant embryos exhibited more dye-labeled motor neurons. These findings suggest that the segregation of the spinal nerve

fibers into the dorsal and ventral nerve groups within the limbs is not severely disorganized in the neuropilin mutant embryos.

Central Olfactory Projection Is Normal in Neuropilin Mutants

Mitral cell axons are major neuropilin-expressing fibers in the CNS in mice (Kawakami et al., 1996). In normal development, mitral cell axons start to grow out from the olfactory bulb at around 12.5 dpc and follow a specific path within the telencephalon to form a fiber tract referred to as the lateral olfactory tract (LOT) (Sugisaki et al., 1996). Also, in explant culture of the telencephalon, mitral cell axons can grow into the telencephalon and form a LOT-like fiber tract (Sugisaki et al., 1996). Thus,
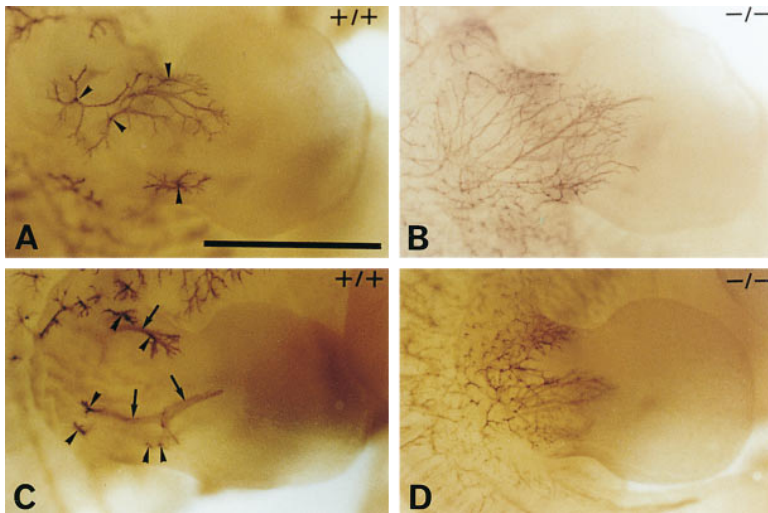
Figure 4. Trajectory of Spinal Nerve Fibers within Limbs

Whole-mount immunostaining with 2H3 of the forelimbs (A and B) and hind limbs (C and D) of the wild-type (+/+) and homozygous mutant (−/−) embryos at 12.5 dpc. Arrows in (C) indicate the major nerve trunks. Arrowheads in (A) and (C) indicate penetration points of the skin-sensory rami. Scale bar (in [A]), 1 mm for (A)–(D).

to examine whether the projection of mitral cell axons is disrupted in the neuropilin mutant embryos, we cultured the telencephalon hemispheres of the wild-type and neuropilin mutant embryos at 12.5 dpc for 3 days on the collagen-coated membrane filters and then labeled the olfactory bulbs with the lipophilic dye DiI. In explant cultures of the mutant embryos as well as of the wild-type embryos, DiI-positive axons formed a LOT-like fiber tract on the surface of the telencephalon. The overall pathway (Figures 6A and 6B) and trajectory (Figures 6C and 6D) of the DiI-labeled olfactory bulb axons were similar between the all wild-type (ten explants [five embryos from four dams]) and homozygous mutant embryos (12 explants [six embryos from four dams]) examined. As mitral cell axons are major components of the LOT in explant culture (Sugisaki et al., 1996), these findings indicate that neuropilin deficiency causes no apparent abnormality in the trajectory or projection of mitral cell axons.

Neuropilin-Deficient DRG Growth Cones Are Protected from Semaphorin III/D-Induced Collapse

More recently, we produced semaphorin III/D mutant mice by targeted disruption of the semaphorin III/D gene (Taniguchi et al., 1997) and found that the PNS efferents of the mutants exhibited abnormalities similar to the neuropilin mutants (see Discussion for details). The similarity in the phenotype between the neuropilin and semaphorin III/D mutants suggests that neuropilin function is correlated with the chemorepellent semaphorin III/D.

To test this possibility, we cultured small explants of DRGs of embryos at 12.5 dpc in the presence of nerve growth factor (NGF) for 14 hr. There were no differences in the number or morphology of DRG neurites between the wild-type and homozygous mutants. Then, we added the culture supernatant of COS7 cells that had been transfected with a semaphorin III/D expression vector (see Experimental Procedures) to the cultures for
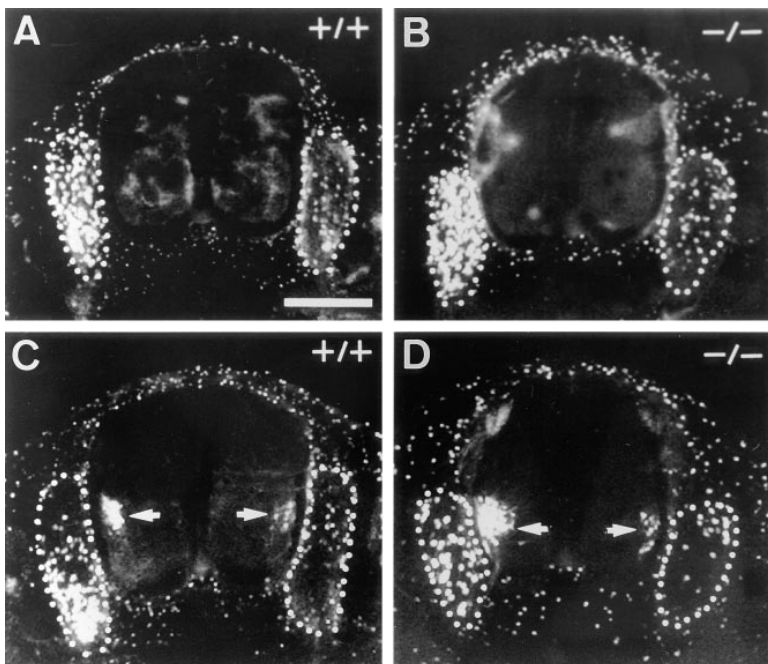

Figure 5. Projection Pattern of Spinal Nerves into Forelimbs

Neurons in the spinal cord and DRGs were retrogradely labeled by application of fluorescein-conjugated dextran onto the forelimbs of the wild-type (+/+) and homozygous mutant (−/−) embryos at 12.5 dpc. In each specimen, the tracer was applied at the dorsal side of the right forelimb (the right side of each figure) and the ventral side of the left forelimb (the left side of each figure). (A and B) The tracer was applied after transection of fibers located at the skin surface (see text). Sensory neurons in DRGs (encircled with dotted lines) but not motor neurons in the spinal cord were labeled with the tracer. Macrophages also incorporated the tracer. (C and D) The tracer was applied after transection of fibers located at deeper parts of the forelimbs (see text). Both motor neurons (arrows) in the spinal motor column and sensory neurons in DRGs are labeled with the tracer. Scale bar (in [A]), 200 μm for (A)–(D).
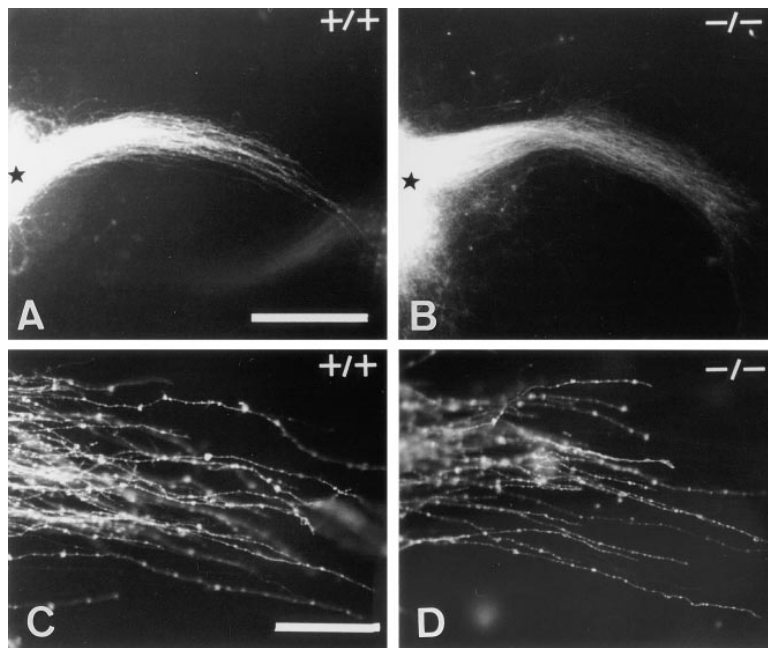
Figure 6. Central Olfactory Projection In Vitro

The telencephalon hemispheres with the olfactory bulb of the wild-type (+/+) and homozygous mutant (−/−) embryos at 12.5 dpc were cultured for 3 days, and then the olfactory bulbs were labeled with the lipophilic dye DiI. (A and B) Pathways of the DiI-labeled olfactory bulb axons within the telencephalon. The asterisks indicate the position of the olfactory bulb. (C and D) Trajectory of the DiI-labeled olfactory bulb axons. Scale bar (in [A]), 200 μm for (A) and (B); (in [C]), 50 μm for (C) and (D).

1 hr. We determined the collapse activity of the culture supernatant and added 80 μl of the culture supernatant to the DRG cultures (1.5 ml of culture medium), which induced a 100% collapse of DRG growth cones. When the culture supernatant was added to the DRG cultures of either the wild-type or heterozygous embryos, 93%–95% of the growth cones collapsed (Figures 7A and 7C), while no collapse was induced on growth cones of the homozygous mutant embryos (Figures 7B and 7C). Under these culture conditions, some growth cones (less than 10% of the total) were not collapsed, even when more culture supernatant was added. Also, 8%–10% of the growth cones exhibited collapse without the culture supernatant (see Figure 7B). Taken collectively, these results indicate that neuropilin-deficient DRG growth

cones are protected from semaphorin III/D-induced collapse.

Discussion

Neuropilin Is Functionally Correlated with a Potent Chemorepellent, Collapsin-1/Semaphorin III/D

Among the members of the collapsin/semaphorin family (for reviews, see Kolodkin, 1996; Püschel, 1996), collapsin-1/semaphorin III/D has well-defined chemorepulsive activity against DRG neurons in vitro (Luo et al., 1993; Messersmith et al., 1995; Püschel et al., 1995, 1996; Shepherd et al., 1996, 1997; Varela-Echavarria et al., 1997). The present growth cone collapse assay clearly demonstrated that neuropilin-deficient DRG growth
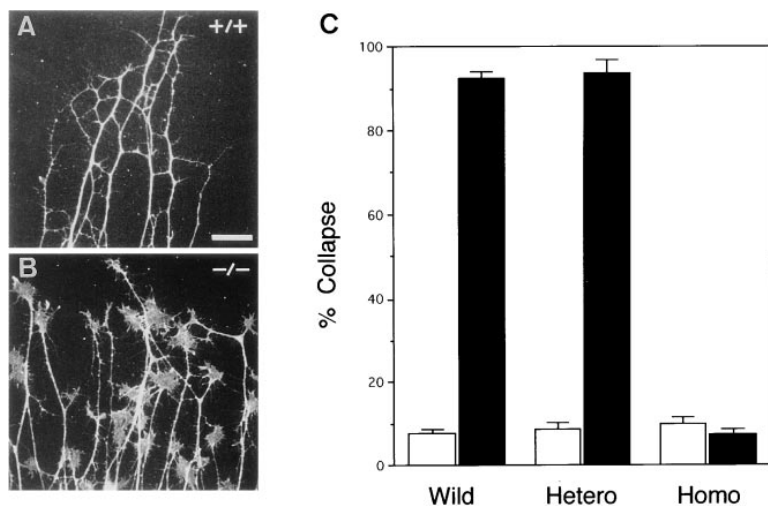

Figure 7. Comparison of Effects of Recombinant Semaphorin III/D on Normal and Neuropilin-Deficient DRG Growth Cones

(A and B) Morphology of DRG growth cones of the wild-type (+/+) and homozygous neuropilin mutant (−/−) embryos in vitro, treated with a sufficient amount of recombinant semaphorin III/D (the culture supernatant of COS7 cells transfected with semaphorin III/D cDNA; see text). The cultures were labeled with fluorescein-conjugated Con A. Scale bar (in [A]), 30 μm for (A) and (B).

(C) Average percentages of collapsed DRG growth cones treated with a sufficient amount of recombinant semaphorin III/D (filled columns) of the wild-type embryo (Wild; 369 growth cones on three explants taken from one embryo), heterozygous embryos (Hetero; 820 growth cones on seven explants taken from four embryos [two dams]), and homozygous mutants (Homo; 917 growth cones on seven explants taken from four embryos [two dams]). Open columns indicate the percentage of collapsed DRG growth cones without recombinant semaphorin III/D of the wild-type embryos (320 growth cones on three explants taken from one embryo), heterozygous embryos (1117 growth cones on six explants taken from four embryos [two dams]), and homozygous mutants (863 growth cones on eight explants taken from four embryos [two dams]). Vertical bars indicate the SEM.

cones were protected from semaphorin III/D-induced collapse, suggesting that neuropilin is functionally correlated with the chemorepellent. Recent two expression cloning studies have shown that neuropilin is a semaphorin III/D-binding protein and that anti-neuropilin antibodies can inhibit the binding of semaphorin III/D to neuropilin as well as the repulsive action of semaphorin III/D on DRG fibers (He and Tessier-Lavigne, 1997; Kolodkin et al., 1997). These results and the present results indicate that neuropilin is an indispensable cell surface component that mediates collapsin-1/semaphorin III/D-induced repulsive and growth cone collapse signals to neurons.

More recently, neuropilin has been shown to bind with other collapsin/semaphorin family members belonging to subfamily III (Feiner et al., 1997; He and Tessier Lavigne, 1997). Moreover, Feiner et al. (1997) have reported that collapsin-1, −2, and -5 bind to neuropilin protein with similar affinities, but each collapsin binds distinct sets of neuropilin-expressing neurons in chick embryos. These findings suggest that neuropilin is a common component of a receptor complex for particular collapsin/semaphorin family members. The unc-33-related cytosolic protein CRMP-62 (Goshima et al., 1995) and rho-related small GTP-binding protein rac-1 (Jin and Strittmatter, 1997) are expected to participate in the intracellular signaling cascade for the collapsin-1-induced growth cone collapse. The cytoplasmic domain of neuropilin protein is highly conserved among vertebrate species (Takagi et al., 1991, 1995; Kawakami et al., 1996; He and Tessier-Lavigne, 1997; Kolodkin et al., 1997) but lacks motifs that potentially participate in cytoplasmic signal transduction. Thus, one hypothesis is that neuropilin forms a complex with additional receptor molecule(s) that is specific for each collapsin/semaphorin member and propagates the collapsin/semaphorin-induced signals into the intracellular signal transduction pathway.

Roles of Neuropilin–Collapsin/Semaphorin-Mediated Signaling in PNS Efferent Projection

In the neuropilin-null mutant mouse embryos, the number, size, and position of the PNS ganglia were almost normal, even though cell packaging in the DRGs was slightly loose, suggesting that the lack of neuropilin expression does not seriously affect differentiation or positioning of PNS neurons. The prominent phenotype of the neuropilin mutant was abnormal trajectory and projection of PNS efferent fibers: neuropilin deficiency caused defasciculation, wide spreading, overshooting their targets, or ectopic projection of the fibers. As these abnormalities were solely detected in PNS fibers in which neuropilin is expressed in normal embryos, they seemed to be the primary effect of neuropilin deficiency from the nerves. Moreover, PNS fibers were able to grow even when they had lost neuropilin, indicating that the lack of neuropilin expression primarily affects nerve fiber guidance but not nerve fiber growth itself.

Behar et al. (1996) produced semaphorin III mutant mice by homologous recombination of the semaphorin III gene and reported abnormal projection of DRG afferent in the mutants. We also produced semaphorin III/D-deficient mice by targeted disruption of the gene in parallel and have shown that the homozygous semaphorin III/D mutant embryos have severe anomalies in PNS efferent projection (Taniguchi et al., 1997). The phenotype in the PNS efferents observed in the present neuropilin mutant mouse embryos is similar to that of the semaphorin III/D mutant mouse embryos in several respects: in both mutants, the ophthalmic nerves overshot, and the distal ends of the cranial nerves, including the maxillary, mandibular, facial, and vagus nerves, were defasciculated and widely spread. Also, a similar abnormal trajectory of the spinal nerves within the limbs was observed in both mutants. These results strongly suggest that chemorepulsive signals that are mediated by neuropilin–semaphorin III/D interaction are a major mechanism in directional guidance of PNS efferent fibers in vivo.

Several studies have shown that semaphorin III/D in mice or collapsin-1 in chicken is expressed in pharyngeal arches, dermamyotome, sclerotome, limb buds at early embryonic stages, and in many mesodermal structures surrounding the PNS efferents at midembryonic stages (Luo et al., 1995; Püschel et al., 1995, 1996; Wright et al., 1995; Giger et al., 1996). The expression patterns of the chemorepellents coincided fairly well with the positions where abnormal trajectories of PNS efferents were found in the neuropilin mutant embryos and also in the semaphorin III/D mutant embryos (Taniguchi et al., 1997). Thus, it is likely that neuropilin-deficient PNS efferent fibers are deprived of their responsiveness to the locally distributed chemorepulsive guidance signals elicited by collapsin-1/semaphorin III/D, drop out from the normal pathways, and grow along with permissive but not specific cues that are distributed widely within embryos, resulting in disorganization of their trajectories.

The present study showed that the fasciculation of PNS efferents and the convergence of spinal nerves into plexus are insufficient in neuropilin-deficient embryos. Similar nerve fiber defasciculation was observed in the grasshopper PNS, when the function of grasshopper semaphorin (G-Sema-I; formerly Fasciclin IV) was perturbed by an anti-G-Sema-I antibody (Kolodkin et al., 1992). Thus, the lack of responsiveness of neuropilin-deficient fibers to semaphorin III/D, which restricts the space for fiber growth, might result in the defasciculation or spreading of the fibers. An alternative explanation for the nerve fiber defasciculation in the neuropilin mutants is that neuropilin directly regulates axon–axon contact. We have shown that neuropilin can mediate cell adhesion by a heterophilic molecular interaction (Takagi et al., 1995). Our previous study of the Xenopus olfactory system (Satoda et al., 1995) suggested that olfactory axon subclasses are sorted within the olfactory nerve, depending on the expression levels of both neuropilin and another cell adhesion molecule, plexin (Ohta et al., 1995). Thus, it might be possible that the deprivation of neuropilin from the PNS efferents reduces axon–axon contact and causes defasciculation of the nerves or insufficient convergence of the spinal nerves into the plexus. The observations that the extent of defasciculation of the spinal nerves is more severe in the neuropilin mutants than in the semaphorin III/D mutants (Taniguchi

et al., 1997) and that cell packaging in the DRGs was loose in the former but not in the latter also support the possibility that neuropilin plays a role in axon–axon or cell–cell contact. The extracellular part of the neuropilin protein is composed of three unique domains, each of which is expected to be involved in molecular interactions (Takagi et al., 1992, 1995; Kawakami et al., 1996), suggesting that neuropilin may interact with cell adhesion ligand(s) as well as chemorepellents.

Overall Pattern of PNS Efferent Projection Is Normal in Neuropilin Mutants

It is of interest that the overall pattern of PNS efferent projection was almost normal in the neuropilin mutants, despite the severely abnormal trajectory of individual fibers: each cranial nerve in the neuropilin mutants projected to the correct pharyngeal arch. The ophthalmic nerve overshot but was limited within its presumptive target region, the front nasal part. Similarly to the normal embryos, the forelimbs of the neuropilin mutant embryos received C4-Th1 spinal nerves. Several studies have shown that the convergence of spinal nerve fibers into the plexus and subsequent fiber sorting and selective fasciculation of different axon classes within developing limbs are essential to establish correct projections of muscle nerves and skin sensory nerves (Tang et al., 1992; Rafuse et al., 1996). However, the present study indicated that, despite the insufficient convergence of the spinal nerves into the plexus and defasciculation of the nerves within the limbs in the neuropilin mutant embryos, the motor axons did not overshoot to the skin surface but were located in deeper parts of the limbs. Also, the segregation of the dorsal and ventral nerve fiber groups within the limbs was apparently normal.

The PNS efferent fibers are stepwise guided by either specific or nonspecific guidance signals derived from their intermediate and final targets (Landmesser, 1984). The present findings suggest that the neuropilin–collapsin/semaphorin-mediated chemorepulsive signal may function as a general but not specific guidance cue and tune the precision of nerve fiber pathways toward their targets, at least in PNS efferent projection. The partial disruption of the segmental pattern of skin sensory projection and overshooting or ectopic projection of PNS sensory fibers observed in the neuropilin mutant embryos may be due to the disorganized trajectory of the fibers. In Drosophila melanogaster, semaphorin II inhibits terminal arborization of motor neurons (Matthes et al., 1995). The present study demonstrated defasciculation and abnormal trajectory of spinal motor axons in the neuropilin-deficient mouse embryos but could not show their projection patterns to muscles. Thus, it is open to question whether neuropilin–collapsin/semaphorin-mediated chemorepulsive signaling plays a role in motor neuron projection.

Roles of Neuropilin in CNS Fibers

Neuropilin is expressed in DRG afferent (Kawakami et al., 1996). Also, several members of the collapsin/semaphorin gene family are expressed in the developing spinal cord (Luo et al., 1995; Püschel et al., 1995, 1996), and semaphorin III/D has been suggested to function

in the patterning of DRG afferent projection within the spinal cord (Messersmith et al., 1995). The present study showed no abnormalities in the pathways and projections of DRG afferent in the neuropilin-deficient embryos at 12.5 dpc, suggesting that the neuropilin–collapsin/semaphorin-mediated chemorepulsive signals do not affect the initiation of sensory afferent inversion into the spinal cord nor the formation of the dorsal funiculus. However, since neuropilin mutants die prior to a developmental stage where differential sensory afferent innervation in the spinal cord can be clearly visualized, it still remains an open question as to whether or not the neuropilin deficiency causes defects in the DRG sensory afferent projection within the spinal cord.

The present study shows that neuropilin deficiency from mitral cell axons caused no abnormalities in the pathway and trajectory of these axons within the telencephalon. The finding coincides well with the previous observation that the growth of olfactory bulb axons in chick embryos was not inhibited by collapsin-1 in vitro, even though a sufficient amount of collapsin-1 is expressed in positions adjacent to the lateral olfactory tract within the telencephalon (Shepherd et al., 1996), suggesting another role of neuropilin than the receptor for chemorepulsive signals. Also, the present findings suggest that neuropilin is not actually involved in fasciculation of mitral cell axons in situ. In the mouse CNS, neuropilin is also expressed in the optic nerve, hippocampal efferent, and middle cerebellar peduncle (Kawakami et al., 1996). Respondence of these neuropilin-expressing fibers to semaphorin III/D or the other collapsin/semaphorin family molecules, however, has not been reported. Further analyses are necessary to clarify the functions of neuropilin in these CNS neurons.

Experimental Procedures

Construction of Targeting Vector

A genomic DNA library was screened with an EcoRI-NotI fragment of the neuropilin cDNA (corresponding to 176th–639th bases of the cDNA; Kawakami et al., 1996), and a 13 kb genomic DNA fragment was obtained that contained an exon encoding the N-terminal half of the a1 domain of the neuropilin protein (corresponding to 421th–595th bases of the neuropilin cDNA; see Kawakami et al., 1996). The 5' 99 bases (429th–527th bases of the neuropilin cDNA) of the exon were deleted, and a XhoI site was inserted into the deleted region. The PGK-neo cassette (neo) was excised with XhoI and SalI from pL2neo (gift from Dr. H. Gu) then spliced into the XhoI site in the deleted exon for positive selection. The targeting vector contained 1.8 kb of homologous sequence upstream of neo. The 1.3 kb XhoI-NotI fragment of the diphtheria toxin A fragment gene cassette (DTA), which was constructed by ligating the 3.6 kb blunted SalI and SphI fragment of pMC1DT-A (Yagi et al., 1993a) and the 0.5 kb SmaI-SphI pgk-poly(A) signal fragment from pGKPuro (Watanabe et al., 1995) was inserted upstream of the neuropilin genome sequence for negative selection. Targeting vector (20 μg) linearized by NotI was electroporated into 1×10^7 TT-2 cells (Yagi et al., 1993b) by use of a gene pulser (250 V, 960 μF) (Bio-Rad). Homologous recombinants were selected by G418 (200 μg/ml), and successful targeting was confirmed by Southern blotting (see below).

Production of Chimeric Mice

Targeted TT-2 ES cells (cell line No. 19) were microinjected into 8-cell stage ICR mouse embryos (Yagi et al., 1993b). The embryos were cultured in M16 medium overnight to blastocysts and were then transplanted into recipient ICR mice. Chimeric mice were crossed with wild-type ICR or C57BL/6 female mice. After two to

three intercrosses of female heterozygous offspring with wild-type ICR or C57BL/6 males, the offspring were crossed to obtain homozygous animals.

Southern Blotting and PCR

Genomic DNA (5 μg) was digested with XbaI, separated on 1% agarose gels, and then blotted onto nitrocellulose filters (Amersham). Hybridization was performed with a 5' flanking probe (see Figure 1B) in 6$\times$ SSC, 5$\times$ Denhardt's solution, 0.1% SDS, 0.1 mg/ml herring sperm DNA overnight at 65°C. The filters were washed with 0.2$\times$ SSC-0.1% SDS solution at 60°C. Genotype analysis of the neuropilin mutants was performed by PCR using primers P1 (5'-CCTCACTGTCTTCTGAAGTGAC-3') corresponding to the 5' flanking region and P2 (5'-GATTTTTATGGTCCCGCCACA-3') matching the deleted part of the exon, and of the P1 and P3 (5'-TGATATTGCT GAAGAGCTTGG-3') corresponding to the neomycin resistance gene (see Figure 1B). Amplification of DNA was performed using Taq DNA polymerase (TaKaRa).

Immunohistochemistry

Whole-mount immunostaining with 2H3 was carried out according to the method reported by Klymkowsky and Hanken (1991). In brief, embryos were fixed with 4% paraformaldehyde in 10 mM PBS (pH 7.0) overnight at 4°C, washed in 0.9% NaCl for 2 hr, and then soaked in 80% methanol series. Endogenous peroxidase activity was quenched with 3% H_2O_2 in Dent's fixative (80% methanol and 20% dimethylsulfoxide [DMSO]) for 3 hr. After washing with Tris-buffered saline containing 1% Tween 20 (TBST) for 3 hr, the embryos were incubated with the antibody 2H3 (1:100 dilution of 2H3 hybridoma culture supernatant with TBST containing 5% skimmed milk, 5% DMSO, and 0.1% sodium azide) for 2 days at room temperature. Then, the embryos were incubated with HRP-coupled anti-mouse Ig antibody (Zymed; 1:200 dilution in TBST containing 5% skimmed milk and 5% DMSO). HRP activity was detected with diaminobenzidine. Cryostat sections (20 μm thick) were collected on poly-L-lysine-coated glass slides and incubated in 2H3 solution overnight at 4°C. Detection of 2H3 was performed with biotinylated anti-mouse Ig antibody (1:200 dilution, Amersham), followed by streptavidin-HRP complex (ABC elite kit, Vectastain).

Labeling of Neurons with Fluorescein-Conjugated Dextran

Embryos were dissected out in Hanks' solution. After making lesions on PNS fibers at appropriate parts of the forelimbs (see text), a small amount of fluorescein-conjugated dextran (dextran, fluorescein, 3000 MW, anionic, lysine fixable; Molecular Probes) was applied. The tracer was dissolved in distilled water, stuck to the tip of a fine tungsten needle, dried, and then applied. The embryos were incubated in a 1:1 mixture of Hanks' solution and Leibovitz L-15 (Flow Laboratories) for 9 hr at 25°C, with continuous bubbling with oxygen. The specimens were fixed with 4% paraformaldehyde, embedded in 3.5% agar, and sectioned (100 μm thick) on a vibratome. The sections were mounted with 90% glycerol and examined under an epifluorecence microscope (Nikon UFX-II).

Organotypic Culture of the Telencephalon and DiI Labeling

Organotypic cultures of telencephalon hemispheres with the olfactory bulb were prepared according to the reported procedures (Sugisaki et al., 1996). The cultures were fixed with 4% paraformaldehyde. Then, a small amount (5 mg/ml solution of 1,1'-dioctadecyl-3,3,3',3'-tetramethylindocarbocyanine perchlorate (DiI, Molecular Probes) dissolved in dimethylformamide was stuck to the tip of a fine tungsten needle and applied to the olfactory bulbs. The specimens were kept in PBS for 7 days at 37°C to fill fibers anterogradely with the dye, mounted with 90% glycerol, and examined under an epifluorecence microscope.

Production of Recombinant Semaphorin III/D

A semaphorin III/D expression vector (pCAG-semIII/D) was constructed as follows. The full length of the protein coding region of the mouse semaphorin III/D cDNA (gene accession number D85028) with a Kozak sequence at its 5' end was ligated into the EcoRI site of the COS cell expression vector pCAGGS (Niwa et al., 1991). COS7 cells were transfected with pCAG-semIII/D using LipofectAMINE

(GIBCO-BRL) and cultured in Dulbecco's modified Eagle's medium (DMEM; Nissui) containing 5% fetal bovine serum (JRH Biosciences) for 4 days at 37°C. Then, culture supernatant was collected.

Detection of Growth Cone Collapse

DRGs at the trunk level of embryos at 12.5 dpc were collected, divided into three to four pieces, and then cultured with DMEM containing 10% fetal bovine serum and 10 ng/ml 2.5S NGF (WAKO). Culture dishes were pretreated with 100 μg/ml poly-L-lysine (Sigma) overnight at 4°C and with 10 μg/ml mouse laminin (GIBCO-BRL) for 2 hr at room temperature. After 14 hr in culture, the supernatant of COS7 cells with or without transfection with pCAG-semIII/D was added to the cultures for 1 hr. The cultures were fixed with 4% paraformaldehyde, washed with PBS containing 0.1% Tween 20, and then labeled with fluorescein-conjugated Con A (EYLABS; 1:50 dilution with TBST).

References

Behar, O., Golden, J.A., Mashimo, H., Schoen, F.J., and Fishman, M.C. (1996). Semaphorin III is needed for normal patterning and growth of nerves, bones and heart. Nature 383, 525–528.

Dodd, J., Morton, S.B., Karagogeos, D., Yamamoto, M., and Jessell, T.M. (1988). Spatial regulation of axonal glycoprotein expression on subsets of embryonic spinal neurons. Neuron 1, 105–116.

Fan, J., and Raper, J.A. (1995). Localized collapsing cues can steer growth cones without inducing their full collapse. Neuron 14, 263–274.

Feiner, L., Koppel, A.M., Kobayashi, H., and Raper, J. (1997). Secreted chick semaphorins bind recombinant neuropilin with similar affinities but different subsets of neurons in situ. Neuron 19, 539–545.

Fujisawa, H., Takagi, S., and Hirata, T. (1995). Growth-associated expression of a membrane protein, neuropilin, in Xenopus optic nerve fibers. Dev. Neurosci. 17, 343–349.

Giger, R.J., Wolfer, D.P., De Wit, G.M.J., and Verhaagen, J. (1996). Anatomy of rat semaphorin III/collapsin-1 mRNA expression and relationship to developing nerve tracts during neuroembryogenesis. J. Comp. Neurol. 375, 378–392.

Goodman, C.S. (1996). Mechanisms and molecules that control growth cone guidance. Annu. Rev. Neurosci. 19, 341–377.

Goodman, C.S., and Shatz, C.J. (1993). Developmental mechanisms that generate precise patterns of neuronal connectivity. Cell 72/ Neuron 10 (Suppl.), 77–98.

Goshima, Y., Nakamura, F., Strittmatter, P., and Strittmatter, S.M. (1995). Collapsin-induced growth cone collapse mediated by an intracellular protein related to UNC-33. Nature 376, 509–514.

He, Z., and Tessier-Lavigne, M. (1997). Neuropilin is a receptor for the axonal chemorepellent semaphorin III. Cell 90, 739–751.

Hirata, T., Takagi, S., and Fujisawa, H. (1993). The membrane protein A5, a putative neuronal recognition molecule, promotes neurite outgrowth. Neurosci. Res. 17, 159–169.

Jin, Z., and Strittmatter, S.M. (1997). Rac 1 mediates collapsin-1-induced growth cone collapse. J. Neurosci. 17, 6256–6263.

Kawakami, A., Kitsukawa, T., Takagi, S., and Fujisawa, H. (1996). Developmentally regulated expression of a cell surface protein, neuropilin, in the mouse nervous system. J. Neurobiol. 29, 1–17.

Kitsukawa, T., Shimono, A., Kawakami, A., Kondoh, H., and Fujisawa, H. (1995). Overexpression of a membrane protein, neuropilin, in chimeric mice causes anomalies in the cardiovascular system, nervous system and limb. Development *121*, 4309–4318.

Klymkowsky, M.W., and Hanken, J. (1991). Whole-mount staining of *Xenopus* and other vertebrates. Meth. Cell Biol. *36*, 419–441.

Kolodkin, A.L. (1996). Semaphorins: mediators of repulsive growth cone guidance. Trends Cell Biol. *6*, 15–22.

Kolodkin, A.L., Matthes, D.J., O'Conner, T.P., Patel, N.H., Admon, A., Bentley, D., and Goodman, C.S. (1992). Fasciclin IV: sequence, expression, and function during growth cone guidance in the grasshopper embryo. Neuron *9*, 831–845.

Kolodkin, A.L., Matthes, D.J., and Goodman, C.S. (1993). The semaphorin genes encode a family of transmenbrane and secreted growth cone guidance molecules. Cell *75*, 1389–1399.

Kolodkin, A.L., Levengood, D.V., Rowe, E.G., Tai, Y.-T., Giger, R.J., and Ginty, D.D. (1997). Neuropilin is a semaphorin III receptor. Cell *90*, 753–762.

Lance-Jones, C., and Dias, M. (1991). The influence of presumptive limb connective tissue on motoneuron axon guidance. Dev. Biol. *143*, 93–110.

Lance-Jones, C., and Landmesser, L. (1980). Motoneuron projection patterns in chick hind limbs following partial reversals of the spinal cord. J. Physiol. *302*, 581–602.

Landmesser, L. (1984). The development of specific motor pathways in the chick embryo. Trends Neurosci. *7*, 336–339.

Luo, Y., Raible, D., and Raper, J.A. (1993). Collapsin: a protein in brain that induces the collapse and paralysis of neuronal growth cones. Cell *75*, 217–227.

Luo, Y., Shepherd, I., Li, J., Renzi, M.J., Chang, S., and Raper, J.A. (1995). A family of molecules related to collapsin in the embryonic chick nervous system. Neuron *14*, 1131–1140.

Matthes, D.J., Sink, H., Kolodkin, A.L., and Goodman, C.S. (1995). Semaphorin II can function as a selective inhibitor of specific synaptic arborizations. Cell *81*, 631–639.

Messersmith, E.K., Leonardo, E.D., Shatz, C.J., Tessier-Lavigne, M., Goodman, C.S., and Kolodkin, A.L. (1995). Semaphorin III can function as a selective chemorepellent to pattern sensory projections in the spinal cord. Neuron *14*, 949–959.

Niwa, H., Yamamura, K., and Miyazaki, J. (1991). Efficient selection for high-expression transfectants with a novel eukaryotic vector. Gene *108*, 193–199.

Ohta, K., Mizutani, A., Kawakami, A., Murakami, Y., Kasuya, Y., Takagi, S., and Fujisawa, H. (1995). Plexin: a novel neuronal cell surface molecule that mediates cell adhesion via a homophilic binding mechanism in the presence of calcium ions. Neuron *14*, 1189–1199.

Püschel, A.W. (1996). The semaphorins: a family of axonal guidance molecules? Eur. J. Neurosci. *8*, 1317–1321.

Püschel, A.W., Adams, R.H., and Betz, H. (1995). Murine semaphorin D/collapsin is a member of a diverse gene family and creates domains inhibitory for axonal extension. Neuron *14*, 941–948.

Püschel, A.W., Adams, R.H., and Betz, H. (1996). The sensory innervation of the mouse spinal cord may be patterned by differential expression of and differential responsiveness to semaphorins. Mol. Cell. Neurosci. *7*, 419–431.

Rafuse, V.F., Milner, L.D., and Landmesser, L.T. (1996). Selective innervation of fast and slow muscle regions during early chick neuromuscular development. J. Neurosci. *16*, 6846–6877.

Rutishauser, U., and Jessell, T.M. (1988). Cell adhesion molecules in vertebrate neural development. Physiol. Rev. *68*, 819–857.

Satoda, M., Takagi, S., Ohta, K., Hirata, T., and Fujisawa, H. (1995). Differential expression of two cell surface proteins, neuropilin and plexin, in *Xenopus* olfactory axon subclasses. J. Neurosci. *15*, 942–955.

Scott, S.A. (1986). Skin sensory innervation patterns in embryonic chick hindlimb following dorsal root ganglion reversals. J. Neurobiol. *17*, 649–668.

Shepherd, I., Luo, Y., Raper, J.A., and Chang, S. (1996). The distribution of collapsin-1 mRNA in the developing chick nervous system. Dev. Biol. *173*, 185–199.

Shepherd, I.T., Luo, Y., Lefcort, F., Reichardt, L.F., and Raper, J.A. (1997). A sensory axon repellent secreted from ventral spinal cord explants is neutralized by antibodies raised against collapsin-1. Development *124*, 1377–1385.

Sugisaki, N., Hirata, T., Naruse, I., Kawakami, A., Kitsukawa, T., and Fujisawa, H. (1996). Positional cues that are strictly localized in the telencephalon induce preferential growth of mitral cell axons. J. Neurobiol. *29*, 127–137.

Takagi, S., Tsuji, T., Amagai, T., Takamatsu, T., and Fujisawa, H. (1987). Specific cell surface labels in the visual centers of *Xenopus laevis* tadpole identified using monoclonal antibodies. Dev. Biol. *122*, 90–100.

Takagi, S., Hirata, T., Agata, K., Mochii, M., Eguchi, G., and Fujisawa, H. (1991). The A5 antigen, a candidate for the neuronal recognition molecule, has homologies to complement components and coagulation factors. Neuron *7*, 295–307.

Takagi, S., Kasuya, Y., Shimizu, M., Matsuura, T., Tsuboi, M., Kawakami, A., and Fujisawa, H. (1995). Expression of a cell adhesion molecule, neuropilin, in the developing chick nervous system. Dev. Biol. *170*, 207–222.

Tang, J., Rutishauser, U., and Landmesser, L. (1992). Polysialic acid regulates growth cone behavior during sorting of motor axons in the plexus region. Neuron *8*, 1031–1044.

Taniguchi, M., Yuasa, S., Fujisawa, H., Naruse, I., Saga, S., Mishina, M., and Yagi, T. (1997). Disruption of semaphorin III/D gene causes severe abnormality in peripheral nerve projection. Neuron *19*, 519–530.

Tessier-Lavigne, M., and Goodman, C.S. (1996). The molecular biology of axon guidance. Science *274*, 1123–1133.

Tosney, K.W. (1988). Proximal tissues and patterned neurite outgrowth at the lumbosacral level of the chick embryo: partial and complete deletion of the somite. Dev. Biol. *127*, 266–286.

Tsuchida, T., Ensini, M., Morton, S.B., Baldassare, M., Edlund, T., Jessell, T.M., and Pfaff, S.L. (1994). Topographic organization of embryonic motor neurons defined by expression of LIM homeobox genes. Cell *79*, 957–970.

Varela-Echavarria, A., Tucker, A., Püschel, A.W., and Guthrie, S. (1997). Motor axon subpopulations respond differentially to the chemorepellents netrin-1 and semaphorin D. Neuron *18*, 193–207.

Watanabe, S., Kai, N., Yasuda, M., Kohmura, N., Sanbo, M., Mishina, M., and Yagi, T. (1995). Stable production of mutant mice from double gene converted ES cells with puromycin and neomycin. Biochem. Biophys. Res. Commun. *213*, 130–137.

Wright, D.E., White, F.A., Gerfen, R.W., Silos-Santiago, I., and Snider, W.D. (1995). The guidance molecule semaphorin III is expressed in regions of spinal cord and periphery avoided by growing sensory axons. J. Comp. Neurol. *361*, 321–333.

Yagi, T., Nada, S., Watanabe, N., Tamemoto, H., Kohmura, N., Ikawa, Y., and Aizawa, S. (1993a). A novel negative selection for homologous recombinants using diphtheria toxin A fragment gene. Anal. Biochem. *214*, 77–86.

Yagi, T., Tokunaga, T., Furuta, Y., Nada, S., Yoshida, M., Tsukada, T., Saga, Y., Takeda, N., Ikawa, Y., and Aizawa, S. (1993b). A novel ES cell line, TT2, with high germline-differentiating potency. Anal. Biochem. *214*, 70–76.